J Appl Electrochem (2010) 40:1807–1816
DOI 10.1007/s10800-010-0112-z

ORIGINAL PAPER

Diamond electrodes for electrochemical analysis

Yasuaki Einaga

Received: 15 January 2010 / Accepted: 15 March 2010 / Published online: 30 March 2010

1 Introduction

Conductive boron-doped diamond (BDD) is an alternative to traditional carbon electrodes that provides superior chemical and dimensional stability, low background currents, and a very wide potential window of water stability. Recently, electrochemical applications using BDD electrodes are attracting much attention in many fields, not only in electrochemistry but also in fields such as functional materials science, analytical chemistry, environmental science, biomedical or biological science and so on [1–5]. In fact, waste water treatment systems, ozone or fluorine generation systems, using BDD electrodes have already become commercially available, and the number of publications involving BDD electrochemistry research is drastically increasing year by year.

In this paper, several examples of electroanalytical applications using polycrystalline BDD electrodes will be shown. Furthermore, some examples using modified functional BDD electrodes such as ion-implanted BDD, BDD microelectrodes, and the highly sensitive detection of arsenic, dopamine, and glucose, will be introduced.

2 Preparation of BDD electrodes [6]

The BDD electrodes were deposited on Si (100) wafers in a microwave plasma-assisted chemical vapor deposition system (ASTeX Corp.). The vapor of liquid mixtures of acetone and trimethoxyborane ($B(OCH_3)_3$) as the source gases were introduced into the reactor by bubbling with hydrogen gas. The liquid mixtures were prepared with appropriate mixing ratios based on Raoult's law so that the boron/carbon (B/C) ratios in the reactor were controlled. The typical grain size of the resulting BDD thin films was up to $\sim$5 μm, with a thickness of $\sim$20 μm for a deposition time of 7 h using 5 kW of plasma power.

Y. Einaga (✉)
Department of Chemistry, Keio University, 3-14-1 Hiyoshi, Yokohama 223-8522, Japan
e-mail: einaga@chem.keio.ac.jp

3 Electrochemical properties of BDD as electrode materials

BDD electrodes have an extremely wide potential window of water stability, low background currents (Fig. 1), chemical and mechanical stability, resistance to fouling, lack of a surface oxide film, and controllable surface termination. These characteristics have led to the application of BDD electrodes in electrochemical sensing, in electroanalysis, in electrochemical synthesis, and for the anodic destruction of organic wastes. BDD also can be used as a transparent, conducting medium for analytical chemistry and photoelectrochemical applications.

4 Applications in electrochemical analysis using polycrystalline BDD electrodes

4.1 Free chlorine [7]

Chlorine is a strong oxidizing agent and is the conventional chemical used for the continuous disinfection of drinking water, water in swimming pools and wastewater [8]. The ability of chlorine to disinfect depends on its concentration. If the concentration is too small, the disinfectant effect is insufficient; however, too much chlorine is wasteful and

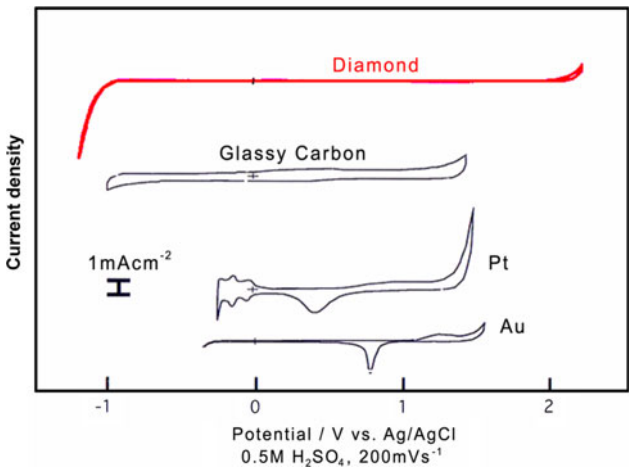

Fig. 1 Electrochemical properties of various electrodes

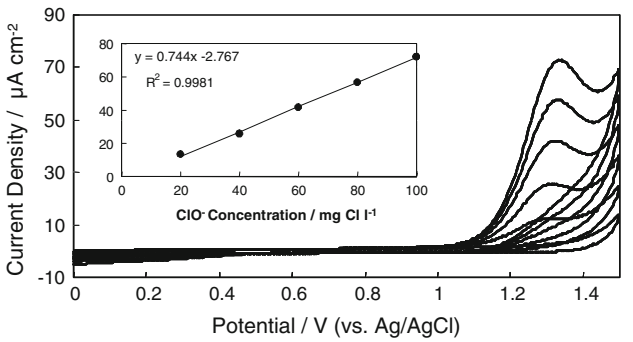

Fig. 2 Cyclic voltammograms of a 0.1 M $NaClO_4$ solution in the presence of various concentrations of free chlorine (2–100 mg Cl L^{-1}) at as-deposited diamond electrodes. Linear calibration plots are shown in the inset (from Ref. [7] Copyright 2008 Elsevier)

creates other dangerous side products such as trihalomethanes. The WHO drinking water standard states that 2–3 mg L^{-1} chlorine gives satisfactory disinfection and residual concentration, where the maximum amount of chlorine allowed is 5 mg L^{-1}. Therefore, the exact determination and continuous on-line monitoring of residual water disinfectant is a strict requirement.

The general detection methods for free chlorine include the colorimetric method, the amperometric titration method, and iodometry. However, these methods are unsuitable for continuous on-line monitoring, because they each have a number of disadvantages, such as the requirement for many types of reagents that may produce greater toxicity, high detection limits, difficulty of operation, etc.

Electroanalytical methods require fewer reagents, promote easy handling and can provide high sensitivity as well as long-term response stability. The reduction of HClO and ClO^- has mainly been reported for the electrochemical determination of free chlorine. However, there are several problems that should be considered when using this method, such as interference, due to a similar reduction potential to that of dissolved oxygen, metal deposition from the sample solution at the electrode, and the effect of trace metal ions. On the other hand, there have been few investigations on quantitative determination based on the anodic reaction of free chlorine, which should be superior, because it is not subject to the above problems.

In the present study, we focused on the quantitative determination and the possibility of continuous on-line monitoring of free chlorine oxidation using BDD electrodes.

Cyclic voltammograms (CVs) for various concentrations of NaClO in a 0.1 M $NaClO_4$ obtained at a scan rate of 100 mV s^{-1} using an as-deposited (ad) BDD electrode are shown in Fig. 2. A well-defined irreversible oxidation peak was observed at a potential of ca. 1.4 V (vs. Ag/AgCl). This is the typical advantage of wide potential window, because the observation of oxidation current at such high potential is impossible in the case of other conventional electrodes due to the narrow potential window. The inset in Fig. 2 shows a plot of the oxidation peak current versus the free chlorine concentration. A linear calibration curve ($r^2 = 0.999$) obtained in the concentration range of 20–100 mg Cl L^{-1}, indicating that determination of free chlorine can be performed at ad-BDD electrodes. A slope of 0.744 µA cm^{-2} mg^{-1} L shows the sensitivity. This sensitivity was 3–4 times higher in comparison with those at conventional electrodes, suggesting the superiority of using ad-BDD for chlorine oxidation. A background current of 3 µA cm^{-2} was obtained, which is very small in comparison with that at a Pt electrode under the same conditions (115 µA cm^{-2}). It is known that BDD electrodes have extremely small background currents due to the inert surface. The small background current can give rise to a very low detection limit due to the decrease in the noise. Furthermore, excellent stability was also shown for repetitive voltammograms.

4.2 Oxalic acid [9]

Oxalic acid, which exists naturally in many plants (spinach, ginger, chocolate, etc.), combines with Ca, Fe, Na, Mg or K to form poorly soluble oxalate salts. High levels in the diet lead to irritation of the digestive system, and particularly of the stomach and kidneys. It is also known to contribute to the formation of kidney stones. The urinary level of oxalic acid has long been recognized as an important indicator for the diagnosis of renal stone formation.

Cyclic voltammetry and flow injection analysis with amperometric detection were used to study the electrochemical reaction. In this case also, the oxidation current was observed at a high potential (ca. 1.35 V vs. Ag/AgCl), which cannot be observed with conventional electrodes. A

good linear response was observed for the concentration range from 50 nM to 10 μM, with an estimated detection limit of ca. 0.5 nM (S/N = 3).

4.3 Proteins

4.3.1 Detection of protein (including cancer markers) [10]

The detection of proteins, including cancer markers, has been attracting increasing attention. The direct, unmediated electron transfer between proteins and electrodes has been studied for many different combinations of proteins and electrode surfaces in recent years. These studies have received much attention because of the requirement in understanding the fundamental reactions of biomolecules, from the viewpoint of developing a direct detection method of the protein at the electrode, or in order to develop new materials by combinations between the protein and the electrode surface. In general, direct electrochemical oxidation of proteins is based on the electrooxidation of metal ions or electroactive amino acids in the protein structure [11]. The proteins studied in this manner range from small, water-soluble redox proteins, to large, sometimes multi-redox enzyme-centered proteins. However, it can be said that the cytochromes, the blue-copper proteins, and the iron-sulfur proteins are as familiar to electrochemical analysts as they are to biochemists. In contrast, the electrochemical detection of the larger non-metalated proteins (e.g., albumin) is reported much less frequently. The limited number of reports is not only due to the complexity of the protein structure but also to the strong adsorption of the proteins on the electrode surface, which can lead to signal depression and resulting lack of predictability and reproducibility.

On the other hand, other superior properties of BDD hydrogen-terminated diamond films are that they are well faceted, hydrophobic, and have a low surface energy. Therefore, it is expected that even proteins can be directly detected electrochemically using BDD because of the surface inertness.

Figure 3a (upper curve) shows the CV of 300 mg dL^{-1} BSA (bovine serum albumin) in 0.1 M phosphate buffered saline (PBS) pH 10 at the BDD electrode. Interestingly, the CV included three peaks. It is known that BSA contains 20 types of amino acids, including cystein, tryptophan and tyrosine, as well as 17 disulfide bonds which are known to be electroactive at BDD electrodes. In order to confirm the active sites of BSA at the BDD electrode, comparison was made between the CVs of BSA and several amino acids (Fig. 3a (lower curves)). The oxidation peaks can be observed separately at different potentials at pH 10. Thus, it is suggested that the oxidation peaks of BSA correspond to the oxidation peaks of cystein, tyrosine and tryptophan.

Further, flow injection analysis (FIA) was used to minimize the adsorbing effects of the protein and to obtain calibration curves (Fig. 3b). The peak current shows good linearity in the concentration range of 5–3000 mg dL^{-1} of BSA, with an experimental detection limit of 5 mg dL^{-1},

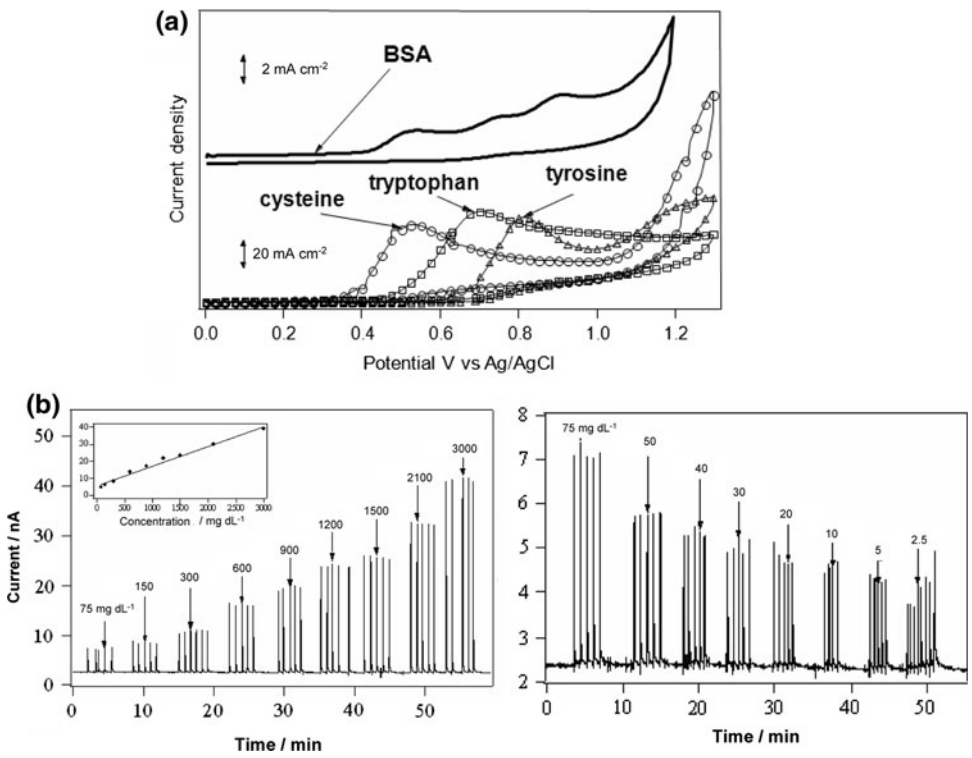

Fig. 3 **a** Cyclic voltammograms of 300 mg dL^{-1} BSA (up) and 1 mM amino acids (bottom) in 0.1 M phosphate buffer solution at diamond electrodes. **b** Signal responses of BSA in various concentrations by using flow injection analysis with a diamond electrode as the detector in the concentration range 75–3000 and 75–2.5 mg dL^{-1}, respectively. The applied potential was 0.8 V vs. Ag/AgCl. The mobile phase was a 0.1 M phosphate buffer solution at pH 7.4. The flow rate was 1 mL min^{-1}. Inset shows linear dynamic concentration of BSA (from Ref. [10] Copyright 2008 Elsevier)

as shown in the linear dynamic calibration in the inset of Fig. 3b. The stability of the current response is also shown for 5 injections of each concentration in the concentration range of 5–3000 mg dL^{-1}. Reproducibility was also confirmed. As an example of cancer maker detection, the possibility of using H-terminated BDD for the direct electrochemical detection of other proteins was also investigated for immunosuppressive acidic protein (IAP). The amperometric FIA responses of IAP showed the possibility of the direct electrochemical detection. A linear detection range of 200–800 μg mL^{-1} was observed. Since the normal human serum IAP level is ~355 μg mL^{-1}, the detectable range should be suitable for cancer screening.

4.3.2 *Detection of conformational change in non-metallo proteins [12]*

Because we knew that the electrochemical direct detection of protein was possible, we established a new electrochemical method for the detection of conformational changes in large, non-metallo proteins such as bovine serum albumin, using flow injection analysis coupled with hydrogen-terminated BDD electrodes.

Protein folding/unfolding is the most fundamental and universal example of biological self-assembly. The sequences of natural proteins have emerged through evolutionary processes such that their unique native states can be found very efficiently even in the complex environment inside a living cell. However, under some conditions proteins fail to fold correctly in living systems, and this failure can result in a wide range of diseases, known as amyloidoses, which includes Alzheimer's disease and Parkinson's disease. Plaques that contain misfolded peptides called amyloid beta are formed in the brain of Alzheimer's disease patients over many years. This protein fold is shared by other peptides such as prions associated with protein misfolding diseases. All known prions induce the formation of an amyloid fold, in which the protein polymerizes into an aggregate consisting of tightly packed beta sheets. Prions cause a number of diseases in a variety of mammals, including bovine spongiform encephalopathy (mad cow disease) in cattle and Creutzfeldt-Jakob disease in humans. Anyway, the detection of denaturation of proteins is very important. For the purpose, denaturation of proteins has been extensively investigated by a number of techniques including nuclear magnetic resonance (NMR), UV-absorption, electron spin resonance (ESR), circular dichroism, birefringence and fluorescence spectroscopy.

Here, we report the results of an investigation into the detection of conformational changes in a non-metallo protein (albumin) by direct electrochemical oxidation using BDD electrodes.

Urea-induced unfolding of BSA has been studied previously by monitoring the change of its intrinsic fluorescence. Here, to validate our new method, urea-induced denaturation of BSA was monitored by both fluorescence and FIA.

To make a better comparison between fluorescence and electrochemistry, the reciprocal of the oxidation current is used as an indicator for the state of protein unfolding and is plotted. Figure 4 shows the changes of fluorescence intensities and reciprocals of oxidation currents by FIA using BDD electrodes at several oxidation potentials as a function of urea concentration. That is, direct electrochemical detection of conformation changes of proteins using BDD electrodes can be performed with advantages in terms of simplicity and sensitivity.

4.3.3 *Detection of protein tyrosine kinase activity [13]*

Recently, as a detection of protein function, protein tyrosine kinase (PTKs) activity in human epidermoid carcinoma cells (A431) was also determined by employing a novel electrochemical method using BDD electrodes. A BDD electrode enables the electrochemical oxidation of tyrosine (Tyr), phosphorylated Tyr (Tyr-P) and sulfated Tyr (Tyr-S) in water-based solutions because of the wide potential window. More so, for the detection of kinase activity, poly (Glu-Tyr) modified magnetic beads were used. Linear-sweep voltammograms for the electrochemical detection of PTKs activity were carried out using BDD

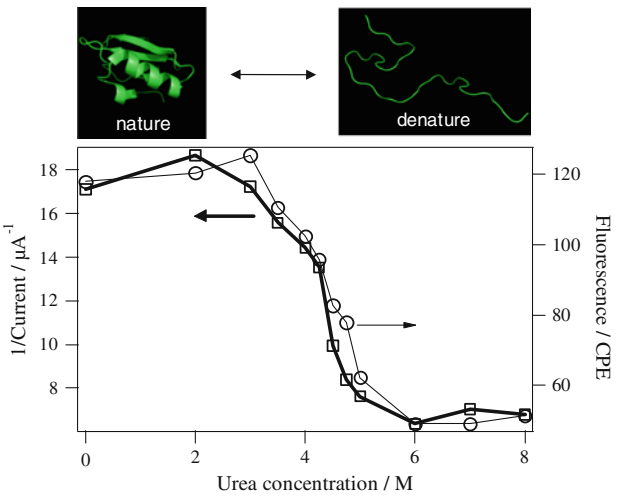

Fig. 4 (*open circle*) Intrinsic fluorescence emission intensity of 50 μg mL^{-1} BSA in 0.1 M phosphate buffer solution (pH 7.4) as a function of urea concentration. Excitation wavelength: 280 nm. Emission wavelength: 290-500 nm. (*open square*) Reciprocal of the oxidation current of 50 μg ml^{-1} BSA in 0.1 M phosphate buffer solution (pH 7.4) as a function of urea concentration. The current is corrected by FIA using BDD electrodes. Oxidation potential is 1300 mV vs Ag/AgCl. Flow rate is 1 mL min^{-1} (from Ref. [12] Copyright 2008 American Chemical Society)

electrodes consisting of peptide-modified magnetic beads. Without phosphorylation of the peptide-modified magnetic beads using PTKs, we observed clear oxidation peaks for Tyr oxidation and no significant electrochemical responses for Tyr-P oxidation at 1.4 V for the back-ground. On the other hand, with phosphorylation of the beads using PTKs, the peak oxidation current at 1.4 V clearly increased, while the peak oxidation current for Tyr oxidation decreased (Fig. 5). This indicates that PTKs activity could be successfully detected by using electrochemical methods employing BDD electrodes. This method was utilized for the in vitro kinase activity detection of human cell lysate, and the electrochemical measurements were compatible with the Enzyme-Linked ImmunoSorbent Assay based method. Our results indicate that the electrochemical method can be applied to real samples such as cell lysate.

4.3.4 Amperometric immunosensor [14]

Furthermore, in order to realize the selectivity of the protein detection, surface modification can be useful. As one example, a poly-o-ABA-modified BDD was developed for a protein immunosensor (Fig. 5). The amperometric sensing of mouse IgG (MIgG) was selected as the model at the poly-o-ABA-modified BDD to compare to the poly-o-ABA-modified glassy carbon (GC) at the same condition. An anti-mouse IgG from goat (GaMIgG) was covalently immobilized at a poly-o-ABA-modified BDD electrode, which used a sandwich-type alkaline phosphatase (ALP) catalyzing amperometric immunoassay with 2-phospho-L-ascorbic acid (AAP) as a substrate. The ALP enzyme conjugated at the immunosensor can generate the electroactive ascorbic acid (AA), which can be determined by amperometric detection. The signal was found to be proportional to the quantity of MIgG. The limit of detection (LOD) of 0.30 ng mL^{-1} (3SD) and 3.50 ng mL^{-1} (3SD) for MIgG at BDD and GC electrodes was obtained. It also was found that the dynamic range of three orders of magnitude (1–1000 ng mL^{-1}) was obtained at BDD, while at GC, the dynamic range was narrower (10–500 ng mL^{-1}). The method was applied to a real mouse serum sample that contained MIgG.

5 Modified functional BDD electrodes

In order to improve the electrochemical properties, several modified types of BDD electrodes were also fabricated.

5.1 Ion-implanted BDD electrodes

5.1.1 Detection of arsenic using Ir-implanted BDD electrodes [15]

Many arsenic compounds are known to be toxic. Their direct exposure to especially humans and animals and the side effects to the ecosystem remain international problems. Arsenic exists in many different chemical forms in nature; particularly, in groundwater it is found almost exclusively as arsenite (AsO_2^-, As^{3+}) and arsenate ($HAsO_4^{2-}$, As^{5+}). Arsenite can be converted to arsenate under oxidizing conditions. However, the conversion in either direction is difficult. The reduced species can be found in both oxidized environments and vice versa. Typical targets of arsenic toxicity are the respiratory system, the circulatory system, and the reproductive system. The toxicity of arsenic is greatly dependent on the arsenite level, since arsenite is $\sim$50 times more toxic than arsenate due to its reactions with enzymes in human metabolism. The higher mobility of arsenite in groundwater also accentuates the potential danger compared to arsenate. In addition, arsenite and arsenate are more toxic than organic

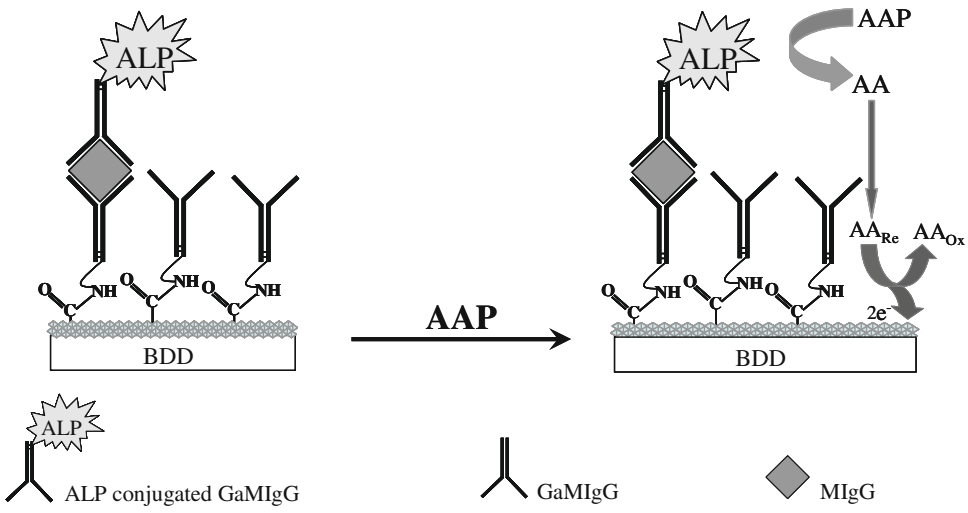

Fig. 5 Schematic of the amperometric enzyme immunosensor based on the poly-o-ABA modified BDD electrode (from Ref. [14] Copyright 2008 American Chemical Society)

arsenic. According to the U.S. Environmental Protection Agency and WHO arsenic guidelines, the maximum contaminant level of arsenic in community water systems is 10 μg L^{-1}.

However, arsenic compounds cannot be detected directly by BDD, because BDD does not have sufficient electrochemical catalytic activity due to the surface inertness. On the other hand, metal electrodes such as iridium have electrochemical catalytic properties, even though the sensitivities are not good due to the large background currents.

Modification of BDD electrodes with redox active particle/compounds offers significant advantages in the design and development of electrochemical sensors. The redox active sites facilitate electron transfer between the substrate electrode and analytes, with a significant reduction in activation overpotential. A wide variety of particles or compounds have been used as electron transfer mediators via modification of BDD surfaces. Preparation of modified diamond by using chemical precipitation and the electrochemical deposition method have been reported. Although electrochemical deposition is a convenient method to prepare metal deposits on substrates, it is not suitable for metal deposition at BDD, because the non-uniform doping of boron in diamond crystals causes the surface conductivity to be inhomogeneous. Furthermore the stability of the deposited metal is not good.

Since its inception, ion implantation has been considered as the most feasible method to change the electrical properties of a diamond substrate. The method modifies the near-surface structure of the target due to the heavy ion bombardment. Here, BDD electrodes modified with implanted iridium ions were investigated for arsenic (III) detection by using cyclic voltammetry (CV) and flow injection analysis (FIA). BDD electrodes were implanted with 800 keV Ir^{+} by using iridium metal powder as the targets. Then, an annealing process was performed at 850 °C for 45 min in a H_2 plasma (80 Torr) to recover the metastable diamond structures.

Cyclic voltammetry and flow injection analysis with amperometric detection were used to study the electrochemical reaction (Fig. 6). The electrodes exhibited high catalytic activity toward As (III) oxidation [16], with the detection limit (S/N = 3), sensitivity, and linearity being 20 nM (1.5 ppb), 93 nA μM^{-1} cm^{-2}, and 0.999, respectively. The precision for 10 replicate determinations of 50 μM As (III) was 4.56% relative standard deviation. The advantageous properties of the electrodes were its inherent stability with a very low background current. The electrode was applicable for the analysis of spiked arsenic in tap water containing a significant amount of various elements in ionic form. The results indicate that metal implantation could be a promising method for controlling the electrochemical properties of diamond electrodes.

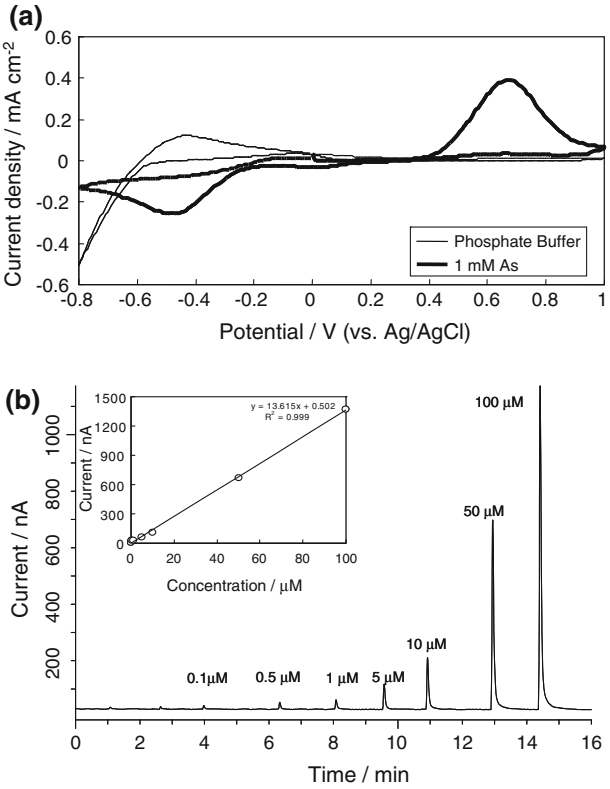

Fig. 6 **a** Cyclic voltammograms of 0.1 M phosphate buffer solution in the absence and presence of 1 mM As(III) at an Ir-implanted BDD electrode. **b** Amperometric response of flow injection analysis using Ir-implanted BDD as a detector. Applied potential was 0.6 V vs. Ag/AgCl. Mobile phase was 0.1 M phosphate buffer solution. Flow rate was 1 mL min^{-1}. Inset shows the variation of current vs. As(III) concentration (from Ref. [15] Copyright 2006 American Chemical Society)

5.1.2 *Selective detection of glucose using Cu-implanted BDD electrodes [17, 18]*

Recently, highly sensitive and simple glucose detection has been considered to be very desirable for the diagnosis and management of diabetes mellitus. However, glucose is normally undetectable using bare BDD electrodes, similar to the above example of arsenic detection. Glucose oxidation is a complex process that requires a catalytic reaction using an enzyme or active metal surfaces. Although Au, Pt, Ni and Cu metal electrodes are known for showing electrocatalysis for glucose oxidation, the BDD electrode does not have catalytic properties. Here, we have studied the electrochemical detection of glucose using Cu-modified BDD electrodes (Cu-BDD). We report the simple technique of selective glucose detection using the Cu-BDD. The selectivity was derived from the differences in the diffusion processes for interfering species such as ascorbic acid (AA) and uric acid (UA) (linear diffusion to the BDD surface) and for glucose (spherical diffusion to implanted copper particles). Each dispersed copper particle of the

Cu-BDD acts as an ultramicroelectrode (UME), because glucose reacts only at the copper surface but not at the BDD surface. On the other hand, interfering substances react at both electrode surfaces. Eventually, the difference of diffusion leads to a dependence or independence of the Faradic current on time, and the steady-state component of the current reflects only glucose concentration. That is, the time dependence of the observed current should be followed by Eqs. 1 and 2, respectively.

Interfering species (linear diffusion):

$$I = nFACD\,(1/\pi Dt) \quad (1)$$

Glucose (sphericaldiffusion):

$$I = nFACD\,(1/\pi Dt + 4/\pi r) \quad (2)$$

Figure 7 (curve a) shows a CV recorded for the oxidation of glucose at Cu-BDD. Figure 7 (curves b and c) show CVs in the absence of glucose at Cu-BDD and in the presence of glucose at a bare BDD electrode respectively. Because no peak was observed in curves (b) and (c), we conclude that glucose was oxidized at the copper surface but not the BDD surface. Furthermore, the copper particles of Cu-BDD act as UMEs for glucose oxidation in the case of low-density modification with Cu, as evidenced by the fact that the curve of the negative scan was superimposed on the positive scan for the Cu-BDD electrodes, while this did not occur for pure metallic Cu electrodes.

Electrochemical quantitative analyses of glucose at Cu-BDD electrodes were carried out by chronoamperometry. A linear calibration curve for the intercepts of Cottrell plots (current vs. inverse square root of time) depending on the glucose concentration was obtained (shown later), indicating that Cu-BDD electrodes can be used as a glucose sensor. On the other hand, CV plots for both AA and UA showed oxidation peaks at ca. +0.2 V vs. Ag/AgCl, and Cottrell plots of the chronoamperometric response at +0.6 V vs. Ag/AgCl exhibited linear curves passing through the origin. These results indicate that the intercepts of the Cottrell plots reflect the glucose concentration at Cu-BDD, even in the presence of interfering substances.

As indicated above, at Cu-BDD, glucose differs from interfering substances in the dimensions of diffusion. Figure 8 shows a schematic illustration of these differences. Glucose could only be oxidized at modified copper with spherical diffusion, while UA and AA could be oxidized at a BDD surface following a linear diffusion process. The Cottrell plots of 6 mM glucose solutions and a mixed solution containing 6 mM glucose and interfering species (0.5 mM AA and 0.5 mM UA) showed similar values for both intercepts.

Electrochemical quantitative analyses of glucose at Cu-BDD electrodes were carried out by chronoamperometry at 0.6 V vs. Ag/AgCl. Figure 9 shows chronoamperograms of 0.2 M NaOH aqueous solutions containing 1–5 mM ($n = 5$) glucose, respectively. Cottrell plots in inset A of Fig. 9 shows that the intercepts were not zero and the slopes were small, indicating that the amperometric response to glucose was at a steady state. A linear calibration curve for the concentration dependence of the intercept value was obtained (Fig. 9 inset B), indicating that Cu-BDD electrodes can be used as a glucose sensor by this method.

Furthermore, Fig. 12 shows the Cottrell plots of 6 mM glucose solution (Fig. 10a) and a mixed solution containing 6 mM glucose and interfering species (0.5 mM AA and 0.5 mM UA) (Fig. 10b). According to the above discussions, similar values for both intercepts reflect the concentration of glucose (6 mM) only. These results suggest that the simple methodology using Cu-BDD could be promising for selective glucose sensors.

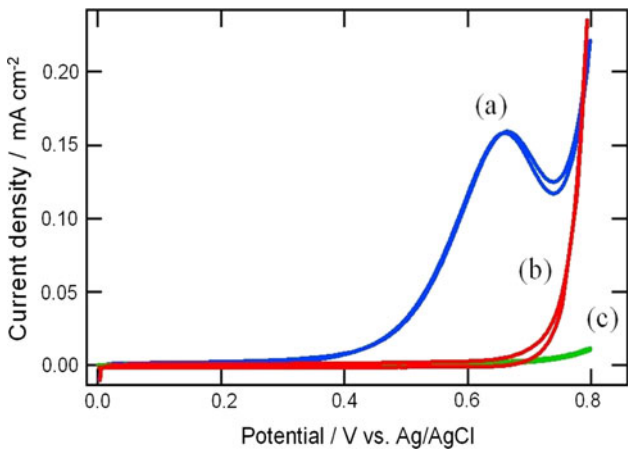

Fig. 7 Cyclic voltammograms of 3 mM glucose in 0.2 M NaOH at the (**c**) diamond electrode, (**a**) Cu-implanted diamond electrode, and (**b**) Cu-implanted diamond electrode in the absence of glucose (from Ref. [17] Copyright 2006 American Chemical Society)

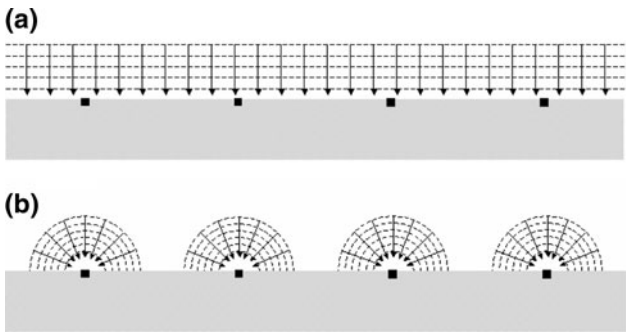

Fig. 8 Illustration of the diffusion profiles at Cu-implanted diamond electrodes for (**a**) ascorbic acid and uric acid and (**b**) glucose (from Ref. [17] Copyright 2006 American Chemical Society)

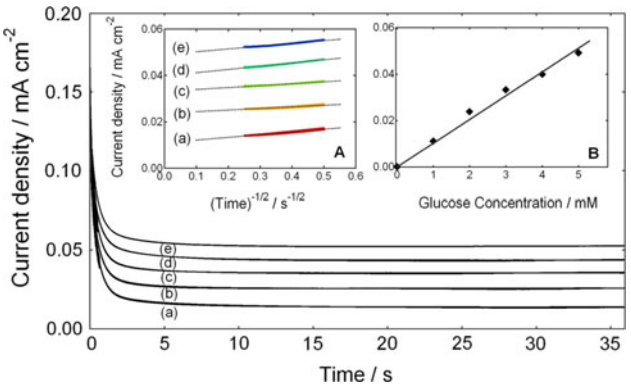

Fig. 9 Chronoamperograms of 1–5 mM (a–e) glucose in 0.2 M NaOH at Cu-implanted diamond electrodes, respectively. The insets show (**A**) related Cottrell plots and (**B**) dependence of current on glucose concentration, extracted from the intercepts of the Cottrell plots. (from Ref. [17] Copyright 2006 American Chemical Society)

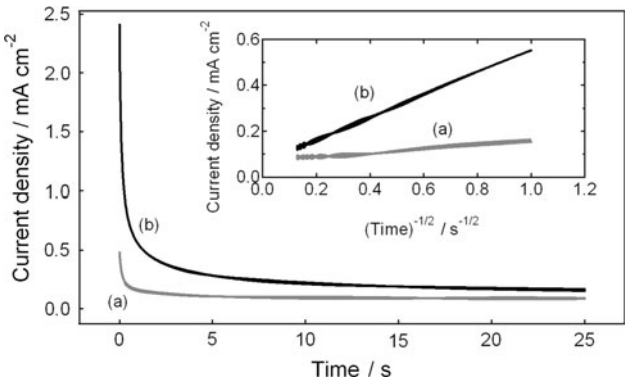

Fig. 10 Chronoamperograms of (**a**) 6 mM glucose and (**b**) a mixture of 0.5 mM ascorbic acid, 0.5 mM uric acid, and 6 mM glucose in 0.5 M NaOH with Cu-implanted diamond electrodes. The *inset* shows their related Cottrell plots (from Ref. [17] Copyright 2006 American Chemical Society)

5.2 Gold-modified BDD-selective detection of As(III) and As(V) by stripping voltammetry [19]

The electrochemical detection of mixed solutions of As^{3+} and As^{5+} has been investigated by stripping voltammetry at gold-modified diamond electrodes. The method was implemented based on the oxidative stripping of As^0 deposited at the electrode surface. Whereas As^{3+} can be deposited by simple electrochemical reduction of As^{3+} to As^0 at −0.4 V (vs. Ag/AgCl), a much more negative potential is required to overcome the activation energy of As^{5+} reduction. However, in such a negative potential region, hydrogen evolution also occurs. Consequently, one more step should be added to release the hydrogen gas adsorbed at the electrode surface during the reduction step. During the deposition of As^{5+}, the As^{3+} species was also simultaneously deposited. Therefore, to differentiate As^{3+} and As^{5+} quantitatively in a mixed solution, both stripping

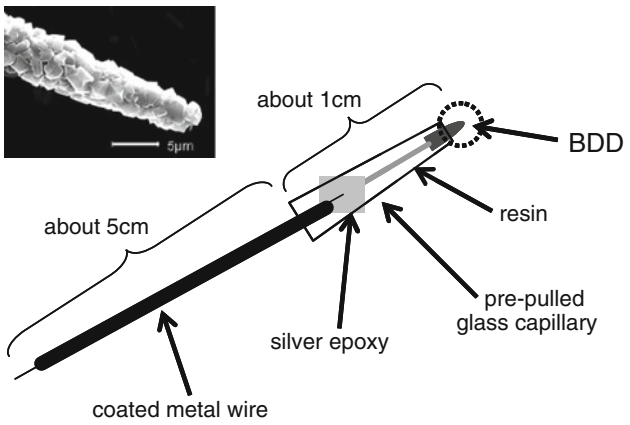

Fig. 11 Schematic drawing of a diamond microelectrode (from Ref. [20] Copyright 2007 American Chemical Society)

voltammetry methods should be performed and compared mathematically. A comparison of stripping voltammograms for both methods for As^{3+} solution in the absence of As^{5+} demonstrated similar peak shapes and current intensities, confirming that errors in the calculation of As^{5+} concentration in the mixed solution with As^{3+} can be avoided. Good linear responses were observed for each standard solution of As^{3+} and As^{5+}. A linear calibration curve could also be achieved for a series of concentrations of 100–1000 ppb As^{5+} in mixed solutions with 100 ppb As^{3+} ($r^2 = 0.99$) and for a series of concentrations of 5–30 ppb As^{3+} in mixed solutions with 100 ppb As^{5+}. Detection limits of 5 and 100 ppb can be achieved for As^{3+} and As^{5+} in mixed solution, respectively. Good reproducibility was shown for stripping voltammetry of As^{3+} and As^{5+} with RSD values ($n = 8$) of 7.5 and 8.4%, respectively. Good stability of gold-modified diamond electrodes before and after arsenic detection was also evaluated by SEM images. Application of the method for real sample analysis was performed for arsenic detection in Yokohama (Japan) tap water.

5.3 In vivo dopamine detection by BDD microelectrodes [20]

The boron-doped diamond (BDD) microelectrode has received much attention as an electrochemical sensor, especially as an in vivo sensor [21–23]. By using this promising electrode, in vivo electrochemical detection of dopamine (DA) was investigated. DA is one of the neurotransmitters, and thought to act as a trigger of many vital activities. Therefore, in vivo DA monitoring is important. However, in the case of the carbon fiber, which is a conventional in vivo sensor, it is a long-standing problem to separate the response from that of some interfering substances, particularly ascorbic acid (AA). To overcome this issue, we used the BDD microelectrode. Anodically

oxidized BDD (ao-BDD) has the property to recognize DA and AA separately by investigating their specificity of oxidation potential [24]. So, we applied this useful property for in vivo analysis with microelectrodes. Finally, a good separation between DA and AA could be obtained not only in vitro but also in vivo. Moreover, some advantages over the conventional carbon fiber electrode were demonstrated. Therefore, we concluded that BDD microelectrodes are highly promising for future in vivo analysis.

BDD thin films were grown on chemically etched tungsten wires (50 μm dia.) by using a microwave plasma-assisted chemical vapor deposition system at a hydrogen pressure of 60 Torr and microwave power of 2.5 kW for 3 h. Boron was doped with a concentration of 10^4 ppm (B/C). A single compartment cell was employed for in vitro electrochemical experiments. Ao-BDD was formed by the electrochemical oxidation of as-deposited, hydrogen terminated, BDD (ad-BDD) at an applied potential of +2.5 V (vs. Ag/AgCl) in 0.1 M HCl for 20 min. In vivo measurements were conducted in a mouse brain. Electric stimulations for the medial forebrain bundle (MFB) were applied to release DA. Square wave pulse voltammetry (SWPV) was used for electrochemical characterization. All experiments were conducted by using an Ag/AgCl electrode as reference and a Pt wire as counter electrode.

Polycrystalline BDD on tungsten wire with the tip diameter of about 5 μm was obtained. This was the smallest among published reports of BDD microelectrodes, and its small size was expected to be workable for in vivo studies without any invasive damage for cells or tissues (Fig. 11 shows a schematic drawing of the diamond microelectrode used for in vivo analysis).

At first, the basic electrochemical properties of BDD microelectrodes were studied in vitro. It was already reported that, at an ao-BDD electrode, the oxidation potential of AA was shifted to a higher potential than that of DA, whereas at ad-BDD, AA was oxidized at almost the same potential as that of DA (i.e., about +0.6 V vs. Ag/AgCl). This is because AA is charged negatively in the aqueous solution, so that electrostatic repulsion is exhibited between the AA and the surface of the ao-BDD macroelectrode, which is terminated with oxygen. Therefore, for the oxidation of AA, much excess potential is needed to approach to the electrode. This behavior was also observed at the ao-BDD microelectrode. Two steps of steady-state current responses appeared for the measurement for the mixture of DA and AA.

Moreover, high sensitivity was obtained, with an experimental detection limit of 50 nM in the presence of AA. This value was adequate for the application for in vivo monitoring of DA.

Based on these observations, an ao-BDD microelectrode was utilized for the in vivo measurements (Fig. 12). The BDD electrode was inserted into the striatum in the mouse brain, and MFB stimulations were applied to induce DA release. Figure 13 shows signal responses following the

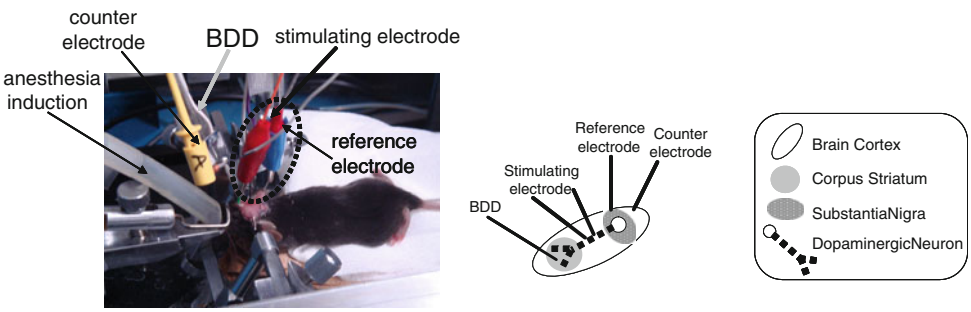

Fig. 12 Photograph and schematic drawing of in vivo mouse brain experimental set up (from Ref. [20] Copyright 2007 American Chemical Society)

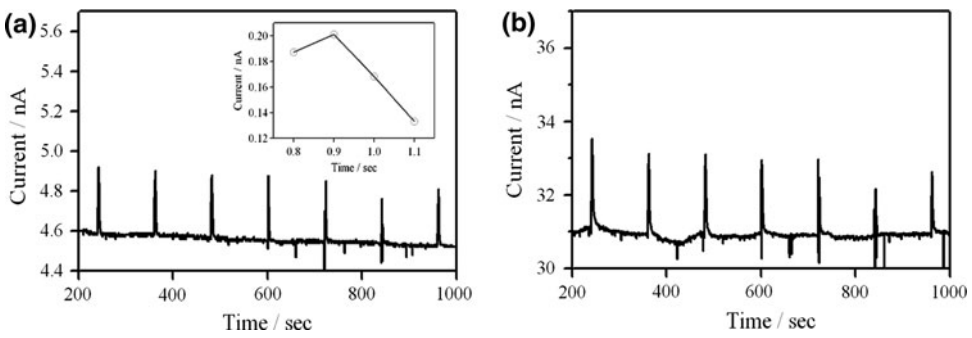

Fig. 13 Differential pulse voltammetry (DPV) monitoring of current response following MFB stimulation (50 Hz, 100 pulses for 2 s) measured at an applied potential of 0.9 V (vs. Ag/AgCl) with (**a**) a diamond microelectrode and (**b**) a carbon fiber electrode. The inset shows the dependence of the signal current on the applied potential. DPV settings: frequency, 50 Hz; potential step, 100 mV; pulse amplitude, 150 mV; starting potential, 0.65 V vs. Ag/AgCl. (from Ref. [20] Copyright 2007 American Chemical Society)

stimulations. Clear signals were recorded for each stimulation and indicated that in vivo monitoring of DA was successfully achieved at the ao-BDD microelectrode. Moreover, a correlation diagram for in vivo analysis showed very similar features to that for in vitro DA. These results confirmed that these signals certainly came from DA oxidation.

6 Summary

We have reported not only the above examples but also several additional examples of sensitive detection by BDD electrodes, such as uric acid [25], NADH [26], acids [27], toxic gases [28], etc. In fact, some of the examples are now in progress for the development of practical electrochemical sensor applications. Furthermore, in order to add other functions and improve the electrochemical properties, BDD electrodes with surfaces chemically modified by functional organic molecules are also actively being developed [29, 30]. Thus, it appears likely that, in the near future, electrochemical sensors using BDD can be applied for environmental analysis and medical analysis.

Acknowledgements The author would like to express thanks to all of co-workers, especially Dr. T. A. Ivandini, Dr. M. Murata, Dr. M. Chiku, Mr. T. Watanabe, Ms. A. Suzuki (Keio University), Dr. K. Yoshimi, and Prof. S. Kitazawa (Juntendo University). I would also like to thank Professor A. Fujishima for his beneficial help and valuable support throughout these works. Finally, I wish to congratulate Professor Christos Comninellis on his 65th happy birthday. He always gave me encouraging and stimulating remarks. His encouragements and heartful suggestions made my research activity fruitful.

References

1. Granger MC, Witek M, Xu J, Wang J, Hupert M, Hanks A, Koppang MD, Butler JE, Lucazeau G, Mermoux M, Strojek JW, Swain GM (2000) Anal Chem 72:3793
2. Fujishima A, Einaga Y, Rao TN, Tryk DA (eds) (2005) Diamond Electrochemistry. BKC Inc and Elsevier
3. Kraft A (2007) J Electrochem Sci 2:355
4. McCreery RL (2008) Chem Rev 108:2646
5. Luong JH, Male KB, Glennon JD (2009) Analyst 134:1965
6. Yano T, Tryk DA, Hashimoto K, Fujishima A (1998) J Electrochem Soc 145:1870
7. Murata M, Ivandini TA, Shibata M, Nomura S, Fujishima A, Einaga Y (2008) J Electroanal Chem 612:29
8. Kodera F, Umeda M, Yamada Y (2005) Anal Chim Acta 537:293
9. Ivandini TA, Rao TN, Fujishima A, Einaga Y (2006) Anal Chem 78:3467
10. Chiku M, Ivandini TA, Kamiya A, Fujishima A, Einaga Y (2008) J Electroanal Chem 612:201
11. Armstrong FA (2002) Encyclopedia Electrochem 9:11
12. Chiku M, Nakamura J, Fujishima A, Einaga Y (2008) Anal Chem 80:5783
13. Chiku M, Horisawa K, Doi N, Yanagawa H, Einaga Y (submitted)
14. Preechaworapun A, Ivandini TA, Suzuki A, Fujishima A, Chailapakul O, Einaga Y (2008) Anal Chem 80:2077
15. Ivandini TA, Sato R, Makide Y, Fujishima A, Einaga Y (2006) Anal Chem 78:6291
16. Salimi A, Hyde ME, Banks CE, Compton RG (2004) Analyst 29:9
17. Watanabe T, Ivandini TA, Makide Y, Fujishima A, Einaga Y (2006) Anal Chem 78:7857
18. Watanabe T, Einaga Y (2009) Biosens Bioelectron 24:2684
19. Yamada D, Ivandini TA, Komatsu M, Fujishima A, Einaga Y (2008) J Electroanal Chem 615:145
20. Suzuki A, Ivandini TA, Yoshimi K, Fujishima A, Oyama G, Nakazato T, Hattori N, Kitazawa S, Einaga Y (2007) Anal Chem 79:8608
21. Sarada BV, Rao TN, Tryk DA, Fujishima A (1999) J Electrochem Soc 146:1469
22. Bond AM (1994) Analyst 119:R1
23. Cahill PS, Walker QD, Finnegan JM, Mickelson GE, Travis ER, Wightman RM (1996) Anal Chem 68:3180
24. Popa E, Notsu H, Miwa T, Tryk DA, Fujishima A (1999) Electrochem Solid State Chem 2:49
25. Popa E, Kubota Y, Tryk DA, Fujishima A (2000) Anal Chem 2:1724
26. Rao TN, Yagi I, Miwa T, Tryk DA, Fujishima A (1999) Anal Chem 71:2506
27. Mitani N, Einaga Y (2009) J Electroanal Chem 626:156
28. Ivandini TA, Yamada D, Watanabe T, Matsuura H, Nakano N, Fujishima A, Einaga Y (submitted)
29. Kondo T, Hoshi H, Honda K, Einaga Y, Fujishima A, Kawai T (2008) J Phys Chem C 112:11887
30. Kondo T, Aoshima S, Hirata K, Honda K, Einaga Y, Fujishima A, Kawai T (2008) Langmuir 24:7545